Inorganic Chemistry

Article

pubs.acs.org/IC

Key Study on the Potential of Hydrazine Bisborane for Solid- and Liquid-State Chemical Hydrogen Storage

Sergii Pylypko,[†] Eddy Petit,[†] Pascal G. Yot,[‡] Fabrice Salles,[‡] Marc Cretin,[†] Philippe Miele,[†] and Umit B. Demirci*,[†]

[†]IEM (Institut Europeen des Membranes), UMR 5635 (CNRS-ENSCM-UM) and [‡]Institut Charles Gerhardt Montpellier, UMR 5253 (UM-CNRS-ENSCM), Universite de Montpellier, Place Eugène Bataillon, F- 34095, Montpellier Cedex 05, France

Supporting Information

ABSTRACT: Hydrazine bisborane $N_2H_4(BH_3)_2$ (HBB; 16.8 wt %) recently re-emerged as a potential hydrogen storage material. However, such potential is controversial: HBB was seen as a hazardous compound up to 2010, but now it would be suitable for hydrogen storage. In this context, we focused on fundamentals of HBB because they are missing in the literature and should help to shed light on its effective potential while taking into consideration any risk. Experimental/computational methods were used to get a complete characterization data sheet, including, e.g., XRD, NMR, FTIR, Raman, TGA, and DSC. From the reported results and discussion, it is concluded that HBB has potential in the field of chemical hydrogen storage given that both thermolytic and hydrolytic dehydrogenations were analyzed. In solid-state chemical hydrogen storage, it cannot be used in the pristine state (risk of explosion during dehydrogenation) but can be used for the synthesis of derivatives with improved dehydrogenation properties. In liquid-state chemical hydrogen storage, it can be studied for room-temperature dehydrogenation, but this requires the development of an active and selective metal-based catalyst. HBB is a thus a candidate for chemical hydrogen storage.

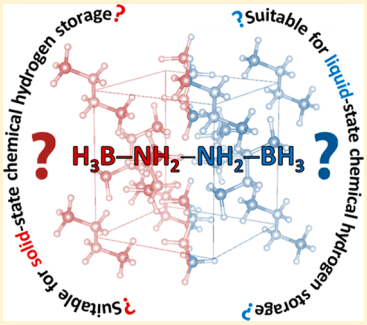

INTRODUCTION

Solid-state chemical hydrogen storage has been shown to be attractive for solving the hydrogen storage issue because materials falling into this category are hydrogen rich. They are considered as hydrogen carriers. Two examples are lithium borohydride $LiBH_4$ (18.5 wt % H) and ammonia borane NH_3BH_3 (19.5 wt % H); they have been widely investigated within the past decade.[1,2] Ammonia borane has attracted particular attention owing to its thermal instability at temperatures as low as 90−110 °C.[2] Notwithstanding, alternative boron- and nitrogen-based materials, most being derivatives of ammonia borane, have recently emerged.

Hydrazine borane $N_2H_4BH_3$ (15.4 wt % H) is one of these alternative materials, envisaged for solid-state chemical hydrogen storage. For example, it was successfully destabilized by addition of lithium hydride taken in an equimolar amount.[3] At that time, little was known about the pristine material, and that is why the synthesis, characterization, and thermal stability of hydrazine borane was investigated in detail.[4] It was especially shown that the pristine material is not suitable for chemical hydrogen storage because of the emission of significant amounts pure hydrazine N_2H_4 and the formation of a shock-sensitive residue upon heating up to 350 °C. In this context, destabilization was envisaged by chemical modification. Hydrazinidoboranes of lithium $LiN_2H_3BH_3$ (11.6 wt % H), sodium $NaN_2H_3BH_3$ (8.9 wt % H), and potassium $KN_2H_3BH_3$ (7.2 wt % H) were prepared by making hydrazine borane and the required alkaline hydride react either by ball milling ($LiN_2H_3BH_3$ and $NaN_2H_3BH_3$) or via a liquid approach ($NaN_2H_3BH_3$ and $KN_2H_3BH_3$).[5] The derivatives showed improved dehydrogenation properties, but it is also worth mentioning that the high reactivity of NaH and KH with $N_2H_4BH_3$ may be problematic for the application potential of the corresponding hydrazinidoboranes.

Hydrazine bisborane $BH_3N_2H_4BH_3$, denoted hereafter HBB (Δ_fH = −251.9 ± 9.2 kJ mol^{-1}),[6] is another example of an alternative boron- and nitrogen-based material with high hydrogen content (16.8 wt % H). HBB may be seen as a derivative of hydrazine borane. It was likely first synthesized in the early 1950s by reaction of diborane with anhydrous hydrazine at 0 °C: Emeléus and Stone reported the formation of a white solid consisting of either hydrazine borane or HBB or both.[7] Though the solid was not well identified, its strong reducing ability and dehydrogenation properties were demonstrated. Another attempt was performed by using similar reactants but at −80 °C. Formation of a white, crystalline, somewhat ether-soluble adduct identified as hydrazine−diborane $N_2H_4{\cdot}B_2H_6$ was reported.[8] Actually, the first article about the unambiguous synthesis of HBB was published in the 1960s by Gunderloy.[9] The experimental conditions were optimized so that the most suitable route was proposed to be the reaction of hydrazine sulfate $[N_2H_5]^+[SO_4H]^-$ with sodium borohydride $NaBH_4$. HBB was however found to be hazardous: it "may explode violently if heated rapidly much beyond 100°C" and "may also be detonated by impact". Though not

Received: March 12, 2015
Published: April 21, 2015

ACS Publications © 2015 American Chemical Society

DOI: 10.1021/acs.inorgchem.5b00569
Inorg. Chem. 2015, 54, 4574−4583

clearly specified, one may guess that such phenomena would occur under inert atmosphere. Further, HBB would be "extremely flammable but not pyrophoric". At that time, but also several years later, HBB was patented by several inventors as gas generator (solid propellant) in the fields of rocketry and inflating system.[10]

More recently, HBB was presented as being suitable for solid-state chemical hydrogen storage. On one hand, Sun et al. investigated thermolysis of HBB and especially stressed on the relatively low temperature of dehydrogenation (ca. 100 °C; heating rates of 2−10 °C min^{-1}) and effective prevention of gaseous byproducts like ammonia and diborane.[11] On the other hand, Li et al. reported enhanced dehydrogenation of HBB in the presence of 2 mol % $NiCl_2$ with, e.g., 8 wt % H_2 liberated within 10 min at 150 °C.[12] None of these reports indicate if there would be any risk with HBB under heating. This is in fact in contradiction with another recent work, since Hügle et al. briefly reported explosive decomposition upon rapid heating and at temperatures over 160 °C.[3]

In fact, HBB has received limited attention within the past decade, and that is why there is little information about fundamentals. Accordingly, we focused on and studied HBB in order to make up for such a gap. We first revisited the synthesis procedure and second characterized both the structural evolution and the properties of this material over a wide range of temperatures. For that purpose, we use various experimental techniques, such as powder diffraction using synchrotron radiation, thermal analysis, NMR, IR, and Raman spectroscopy techniques, combined with computational methods to allow a complete elucidation of the structures. Our primary objective, which is of fundamental importance, was to provide a complete data sheet about HBB. Also, we aimed at getting enough pieces of information to check the suitability of this material for energy applications, namely, solid- and liquid-state chemical hydrogen storage.

RESULTS AND DISCUSSION

Structural Characterization. The successful synthesis of HBB was verified by solution-state NMR spectroscopy on the nucleus ^1H (Figure 1a). The singlet at δ = 6.16 ppm is ascribed to the N_2H_4 moiety, where all of the ^1H elements have similar chemical environments owing to the presence of the two terminal BH_3 groups providing symmetry to the molecule. This is unlike hydrazine borane $N_2H_4BH_3$, where two singlets at δ = 3.44 and 5.45 ppm were found and attributed to the ^1H atoms of N−NH_2 and B−NH_2, respectively.[4] The spectrum also shows the four large signals ascribed to the borane groups, i.e., a quartet of normalized intensity 1:1.4:1.4:1 at δ = 1.92, 1.61, 1.28, and 0.97 ppm, respectively, and centered at δ = 1.45 ppm. This is typical of the heteronuclear coupling between ^{11}B and ^1H for BH_3, with $^1J_{BH}$ equal to 94.6 ± 0.5 Hz. In some respect, HBB shows a B−H coupling region that is similar to that of hydrazine borane $N_2H_4BH_3$ with δ = 0.9−1.9 ppm[4] and comparable to that of ammonia borane NH_3BH_3 with δ = 0.8−2.0 ppm.[13] Also, the B−H coupling constants are equivalent for these three boranes.[4,13] The solution-state $^{11}B\{^1H\}$ NMR spectrum of HBB (Figure 1b) confirmed the presence of the BH_3 group and showed the absence of any other BH_x environments (with $x \leq 3$). The NMR shielding for all of the atoms present in HBB can be determined by DFT calculations (Figure S1 and Tables S1−S3, Supporting Information). The comparison of different DFT codes leads to a good correlation between experimental and simulated

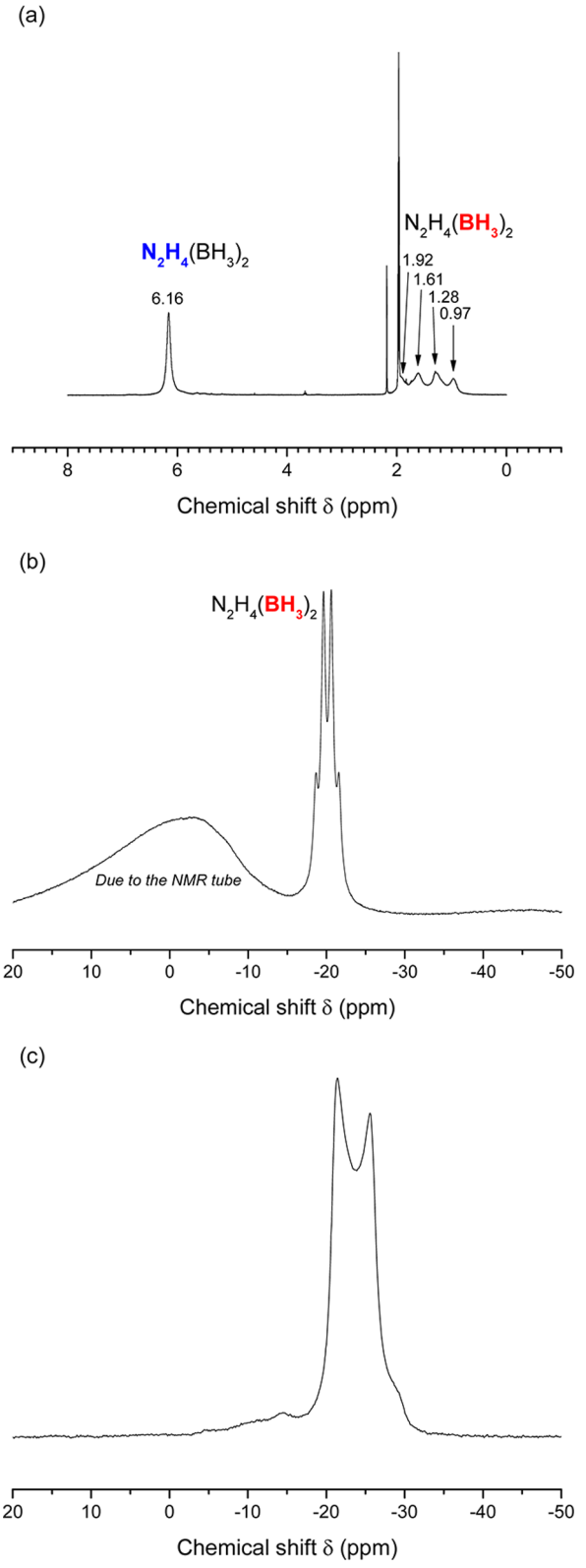

Figure 1. NMR spectra of HBB: (a) solution-state ^1H (CD_3CN, 300.13 MHz, 30 °C); (b) solution-state ^{11}B (D_2O, 96.29 MHz, 30 °C); (c) solid-state ^{11}B recorded at −10 °C (128.37 MHz).

results and allows us to attribute unambiguously each signal to the corresponding atoms.

The chemical structure of HBB was also analyzed by solid-state MAS NMR spectroscopy of the nucleus ^{11}B (Figure 1c).

DOI: 10.1021/acs.inorgchem.5b00569
Inorg. Chem. 2015, 54, 4574−4583

Like for hydrazine borane and ammonia borane,[4,13] there are two observable peaks, centered at $\delta = -24$ ppm, which are due to a quadrupolar coupling. Consistently, the signal can be ascribed to the BH_3 moiety. The sharpness of the peaks is an indication of the high crystallinity of the borane. At higher chemical shifts, over the range from −17 to −3 ppm, the baseline suggests the presence of over BH_x environments (with $x \leq 3$). As not observed in the solution-state $^{11}B\{^1H\}$ NMR spectrum, they are explained by the slight evolution of HBB during the high-speed rotation of the spectrometer rotor.

The IR spectrum of HBB is shown in Figure 2a. It reveals numerous bands with different intensities at wavelengths typical

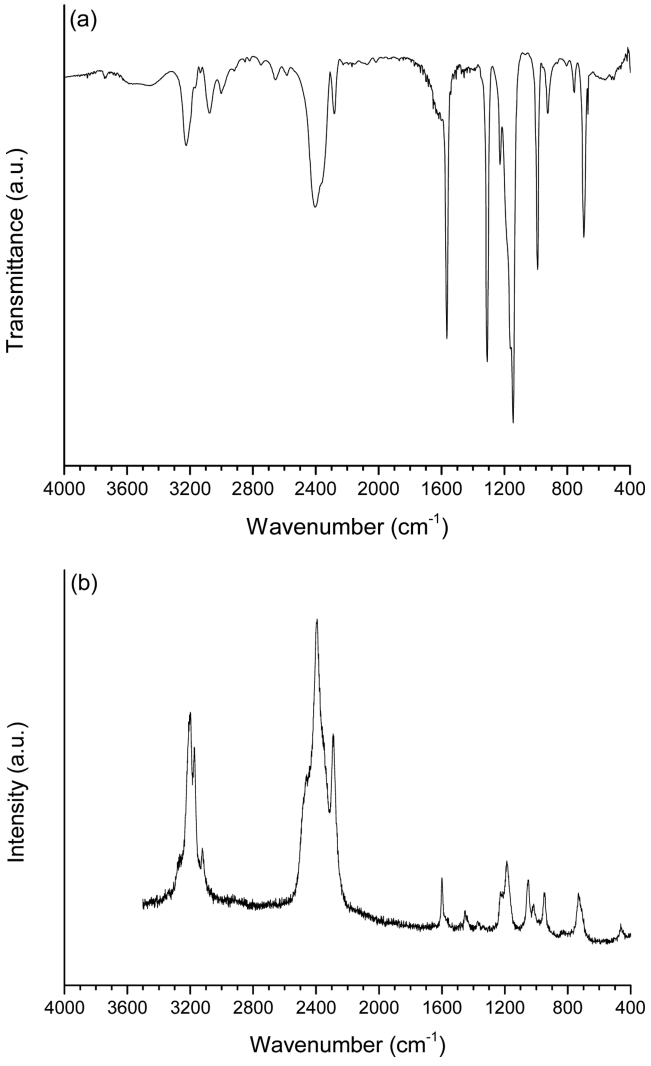

Figure 2. (a) IR and (b) Raman spectra of HBB, recorded in room conditions.

of boron- and nitrogen-based materials.[11−14] The attribution of the bands was performed with the help of this literature and, above all, using molecular calculations (Figures S2−S4, Supporting Information). It is as follows: (i) 3600−2550 cm^{-1} for the N−H symmetric and asymmetric stretching; (ii) 2550−2200 for the B−H symmetric and asymmetric stretching; (iii) 1600−1300 cm^{-1} for the N−H asymmetric and symmetric wagging, respectively, the band at 1310 cm^{-1} being also attributed to the N−N bending; (iv) 1300−1100 cm^{-1} for the B−H wagging and/or rocking; (v) 989 cm^{-1} for the N−H twisting and/or rocking; (vi) 924 cm^{-1} for the B−H twisting or the BN−N asymmetric stretching or the N−N symmetric stretching; (vii) 850−650 cm^{-1} for the B−N and BN−N symmetric stretching. In fact, the IR spectrum favorably compares to previously reported ones, suggesting successful formation of HBB.[11,12]

The Raman spectrum of HBB is shown in Figure 2b. The bands were ascribed with the help of the available literature[15] and, above all, using molecular calculations (Figures S5− S7, Supporting Information). The ascription is as follows: (i) 3300−3100 cm^{-1} for the N−H asymmetric and symmetric stretching; (ii) 2600−2200 cm^{-1} for the B−H asymmetric and symmetric stretching; (iii) 1601 cm^{-1} for the N−H scissoring; (iv) 1455 cm^{-1} for the N−H wagging; (v) 1250−1150 cm^{-1} for the B−H twisting and/or scissoring; (vi) 1100−950 cm^{-1} for the B−H and/or N−H deformation (wagging and/or twisting); (vii) 734 cm^{-1} for the B−N stretching.

Crystallographic Characterization. The crystal structure and thermal behavior of HBB were investigated by X-ray thermodiffractometry over a wide range of temperatures. The structure evolution was investigated during a thermal cycle upon cooling (from room temperature to −192 °C) and upon heating (from −192 to 127 °C) using a 1 °C min^{-1} rate. Heating was stopped at 127 °C to avoid decomposition of the material. Figure 3a and 3b shows the evolution of the diffraction pattern as a function of temperature upon cooling and heating. A phase transformation is first evidenced upon cooling at 10 °C, which corresponds to a phase transition between pristine α-HBB, the room-temperature phase, and α'-HBB, the low-temperature phase. The latter is stable over between 7 and −192 °C. Upon heating, the transformation was found to be reversible and occurs at ca. 17 °C. It is worth noting that the phase transition domain, i.e., the temperature range where the two phases are observed together on the diffraction patterns (patterns in black line), is much larger upon heating with 15 °C than upon cooling with 5 °C (Figure 3c and 3d). These results are consistent with those obtained in the same conditions by DSC (Figure S8, Supporting Information), which permitted us to evaluate a transition energy of ca. 541 J g^{-1} (571 J mol^{-1} upon cooling).

As reported above, HBB presents two crystal structures: α-HBB (room-temperature phase) and α'-HBB (low-temperature phase). These structures were refined from synchrotron X-ray radiation. The XRD pattern of α-HBB at −192 °C has been successfully indexed using an orthorhombic unit cell. Actually, the α' phase at 27 °C crystallizes also in the orthorhombic unit cell with different unit cell parameters. For both, systematic absences were consistent with the *Pbca* (No. 61) space group. The crystal structures have been solved by combining FoX and JANA2006 packages and were refined by the Rietveld method using the JANA2006 package (Tables S4−S7, Figures S9 and S10, Supporting Information). Table 1 summarizes the unit cell parameters of the two phases.

The structure of our phase α-HBB is in contradiction with that proposed by Sun et al. for a sample analyzed in room conditions.[11] Indeed, they found a cubic unit cell with a = 7.662(1) Å, V = 449.8(1) $Å^3$, Z = 4, and space group *P*23 (No. 195). For HBB dioxane solvate $0.5(H_4N_2(BH_3)_2)\cdot O_2C_4H_8$, Mebs et al. reported a orthorhombic crystal structure with space group $P2_1/n$ (No. 14) and the following parameters: Z = 4, a = 8.258(2) Å, b = 8.221(2) Å, c = 10.372(2) Å, β = 94.95(3)°, and V = 701.5(2) $Å^3$.[16]

DOI: 10.1021/acs.inorgchem.5b00569
Inorg. Chem. 2015, 54, 4574−4583

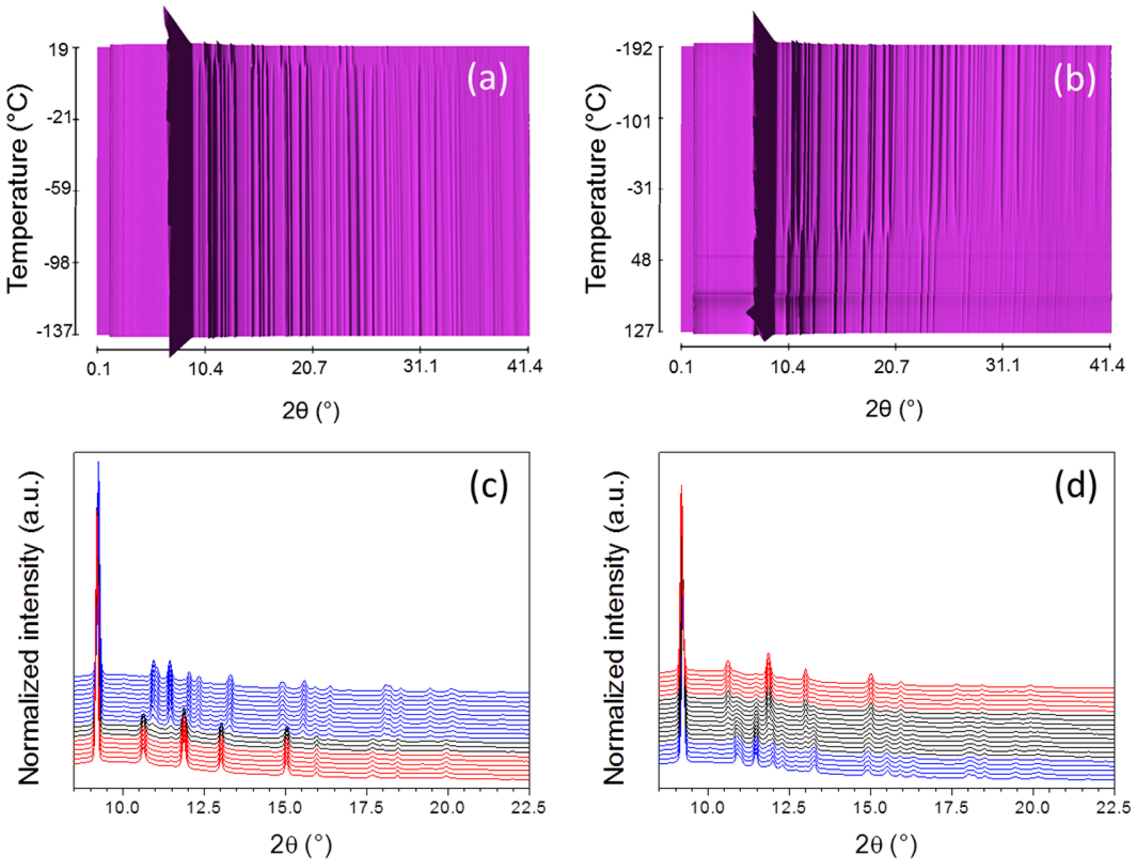

Figure 3. Sequential plot of the diffraction patterns for HBB showing the transition (a) upon cooling and (b) upon heating at ca. 10 and ca. 17 °C, respectively. Waterfall plots of a fragment of the diffraction patterns collected upon (c) cooling and (d) heating between −193 and 127 °C. Patterns in red, black, and blue correspond to α-HBB, a mixture of α- and α'-HBB, and α'-HBB, respectively.

Table 1. Space Group (SG), Unit Cell Parameters, Goodness of Fit, and *R* Values for All Refined Structures α-HBB (Room-Temperature Phase) and α'-HBB (Low-Temperature Phase)

	α-HBB	α'-HBB
formulas	$H_{10}B_2N_2$	$H_{10}B_2N_2$
M_w (g mol^{-1})	59.79	59.79
SG	*Pbca* (No. 61)	*Pbca* (No. 61)
Z	4	4
a (Å)	7.6491(8)	7.2654(4)
b (Å)	7.6909(9)	7.3505 (4)
c (Å)	7.6728(12)	8.1109(5)
V (Å^3)	451.38(10)	433.16(4)
T (°C)	38	−192
ρ_{calcd} (g cm^{-3})	0.8787	0.9157
GoF	9.06	10.64
Rp	0.97	0.94
wRp	1.14	1.20

High-energy X-ray diffraction patterns obtained at the ESRF allowed us to record patterns with more accurate resolution compared to laboratory equipment and then to solve the structures. Figure 4 shows the refined structure of the α-HBB phase. Knowing this structure, the evolution as a function of the thermal stimuli was scrutinized. The cell dimensions were obtained from Le Bail refinement carried out on patterns recorded every 10 °C. The temperature evolution of the unit cell parameters and unit cell volume for the two phases is reported in Figure 5. It can be seen that the influence of the temperature on the unit cell parameters is more important for the low-temperature phase of HBB compared to the room-temperature one. The coefficients of thermal expansion α_0 were found to be close to $18.72(1) \times 10^{-5}$ and $10.86(1) \times 10^{-5}$ K^{-1} for the low-temperature and room-temperature forms, respectively.

The simulated molecular structure proposed in Figure 4 is in agreement with that proposed by Mebs et al. for HBB dioxane solvate.[16] Indeed, for both works, HBB has a chair conformation. Furthermore, DFT calculations performed on clusters with DMol^3, CASTEP, and Gaussian confirmed and led us to obtain very similar structures (Figures S11 and S12, Supporting Information). Such configuration is also obtained in the simulated structure determined from periodic calculations and using the unit cell parameters extracted from the XRD pattern. Such a conformation can be obtained for periodic calculations using low-temperature and room-temperature cell parameters. Further, the distances extracted from the XRD data for the heaviest atoms are very similar to the distances predicted in both the molecule and the periodic models. We can thus conclude that the simulated structures described from the XRD data are consistent with both the periodic and the molecular calculations. However, the simulated molecular structure reported by Sun et al. is different, with a boat conformation, for a cubic HBB.[11]

Additional DFT calculations were performed on the HBB molecule in order to extract the partial charges (Figures 6, S13, and S14, Supporting Information). The presence of hydridic

DOI: 10.1021/acs.inorgchem.5b00569
Inorg. Chem. 2015, 54, 4574−4583

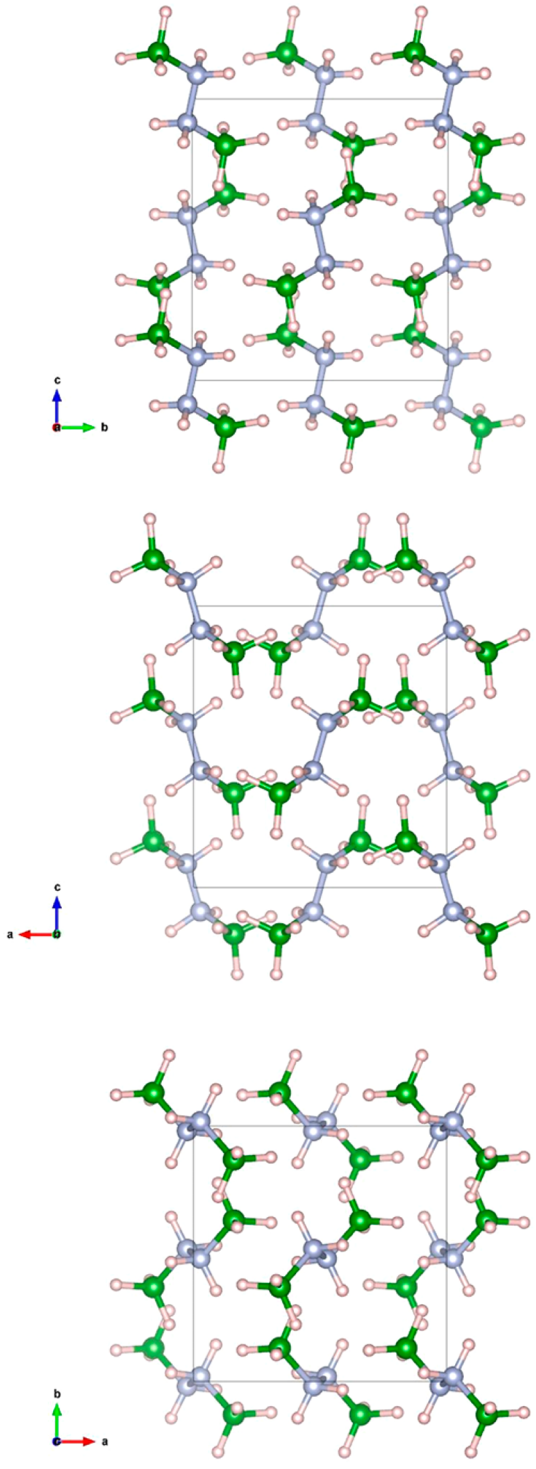

Figure 4. Crystal structure of α-HBB along the [100], [010], and [001] directions. H, B, and N atoms are represented by pink, green, and blue spheres.

and protic hydrogens ($H^{\delta-}$ and $H^{\delta+}$) is confirmed. Such partial charge distribution is evidence of the dihydrogen bonding B–$H^{\delta\alpha}\cdots H^{\delta+}$–N, rationalizing the solid state of the borane in ambient conditions. Also, such partial charge distribution leads us to propose a dehydrogenation process implying one $H^{\delta+}$ and one $H^{\delta-}$ to form the H_2 molecule.[14] Accordingly, the HBB molecule is able to release a maximum of 4 H_2 molecules. Indeed, Sun et al. were able to analyze a dehydrogenated

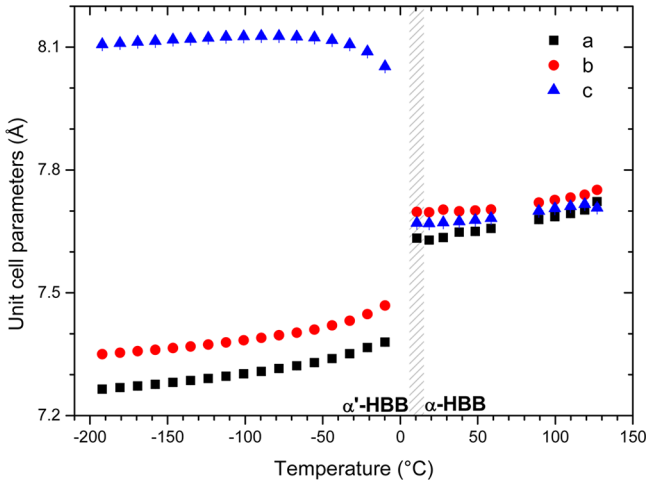

Figure 5. Evolution of the unit cell parameters as a function of the temperature from −192 to 127 °C.

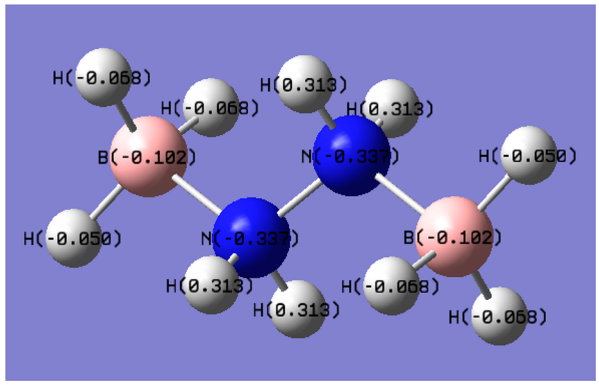

Figure 6. Partial charges extracted from Gaussian calculations following the Mulliken scheme.

product up to 350 °C and reported the formation of $[HBN_2BH]_2$ while taking into account the loss of 4 mol of H_2 per mole of HBB.[11]

Textural Properties and Density. Hydrazine bisborane is a white crystalline powder. A specific surface area of 16 $m^2\ g^{-1}$ was determined by N_2 sorption (−192 °C) and according to Brunauer–Emmett–Teller (BET) theory (Figure S15, Supporting Information). It has a type II adsorption isotherm. This is indicative of a finely divided nonporous solid. The density of HBB was determined by helium pycnometry in ambient conditions. It is 0.955(4) g cm^{-3}. This is higher than the density calculated from the crystal structure. As the pycnometer is kept under air, water adsorption and/or hydrolysis in some extent could explain the difference. Another reason would be the amount of analyzed sample, i.e., <1 g, whereas it is preferable to use more than 2 g to get accurate data.

Thermal Characterization and Gas Analyses. As mentioned in the Introduction, the behavior of HBB under heating is somehow controversial: risk of violent explosion for a sample heated rapidly beyond 100 °C was reported on one side,[3,8] and no unexpected hazardous phenomenon during thermolysis even at a heating rate of 15 °C min^{-1} was reported on the other side.[11,12] With this in mind, we carried out DSC and TGA measurements for α-HBB. Heating rates of 1, 3, 5, and 10 °C min^{-1} were tested for 2–3 mg of sample. The analyses were done over the range 40–400 °C. The DSC

DOI: 10.1021/acs.inorgchem.5b00569
Inorg. Chem. 2015, 54, 4574–4583

measurements were done without problem. However, during one of the TGA measurements, with a 10 °C min^{-1} heat ramp, the sample exploded at around 171 °C (Figure S16, Supporting Information), causing destruction of the furnace. This confirms the hazardous behavior of HBB when heated rapidly.

The thermolytic decomposition of α-HBB was even so investigated by TGA coupled to MS but at a rate lower than 10 °C min^{-1}. The results are shown in Figures 7, S17 and S18,

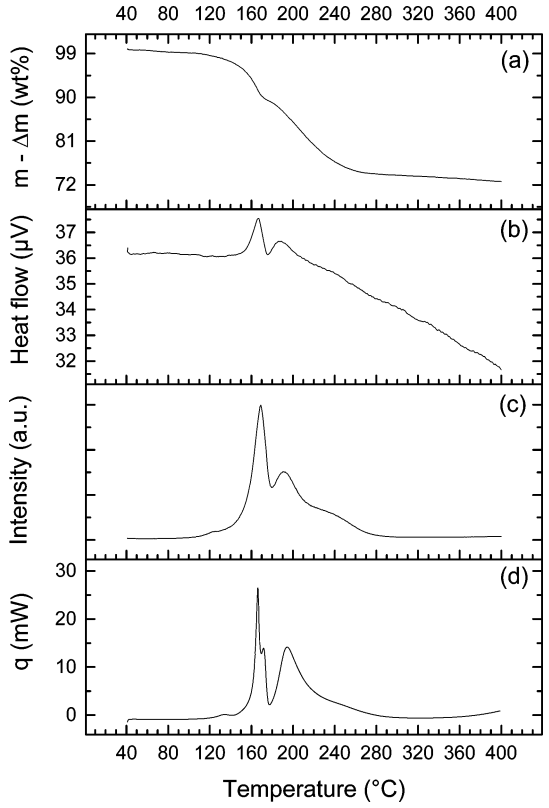

Figure 7. (a) TGA, (b) DTA, (c) H_2 (m/z = 2) evolution, and (d) DSC for α-HBB heated at 5 °C min^{-1} from 40 to 400 °C.

Supporting Information. The decomposition of α-HBB seems to be a complex process. Though the TGA and DTA curves show two successive processes, one can see in the MS spectrum that H_2 evolves according to four successive reactions. The release of H_2 starts since 90 °C, but most is released within the range 140−260 °C, which is not attractive for application when compared to the counterparts ammonia borane and hydrazine borane.[2,4,13] The purity of the evolving H_2 would be much acceptable, with negligible traces of diborane B_2H_6 at 80−100 °C and NH_3 at >240 °C (Figure S18, Supporting Information). Sun et al. reported the release of pure H_2, while only H_2, NH_3, and B_2H_6 were analyzed.[11] In such conditions, our results are in good agreement with Sun et al.'s. The formation of NH_3 was also reported by Fu et al., especially at 252 °C.[17] However, the weight loss found at 400 °C in our conditions is 27.3 wt %, which is almost twice the hydrogen content in HBB (16.8 wt % H). Fu et al. detected the evolution of borazine,[17] but this byproduct was not detected in our conditions. Like for HB,[4] we believe that the aforementioned difference is due to hydrazine N_2H_4. This byproduct has the tendency to condensate onto any cold surface before reaching the MS device, which may explain why no signal for this byproduct can be seen by MS.[4] The release of pure N_2H_4 might be a reason for the explosion.

The thermolytic decomposition of α-HBB was studied by DSC at different heating rates, i.e., 1, 3, 5, and 10 °C min^{-1}. The curves are displayed in Figures 7 and S19, Supporting Information. The complexity of the decomposition of HBB is confirmed. At low heating rate (1 °C min^{-1}), four exothermic signals can be seen, which is consistent with the H_2 evolution curve discussed previously. At high heating rate (3, 5, and 10 °C min^{-1}), a fifth exothermic signal is also distinguished for the first main decomposition signal (assimilated to a splitting), suggesting that the first important decomposition is a two-step process. The apparent activation energy (E_a) of the first decomposition stage was determined with the help of Kissinger's method ($\ln(\beta/T_p^2) = -E_a/(RT_p) + C$, with β being the heating rate, T_p the temperature at which the exothermic signal peaks, and C a constant).[18] We found 134.4 kJ mol^{-1} (Figure S20, Supporting Information). This is consistent with the datum (143.2 kJ mol^{-1}) reported by Li et al. for TPD experiments obtained at 3, 5, 10, and 15 °C min^{-1}.[12] Sun et al. found an energy of 106.4 kJ mol^{-1}, letting them conclude that the first-step dehydrogenation has moderate kinetics.[11]

The thermolytic decomposition of α-HBB (100 mg) was investigated in isothermal conditions (50, 60, 70, 80, and 90 °C) for 7 days, where the pressure variation (i.e., the mole number of H_2) was followed with time. The results are shown in Figure 8. At temperatures of 50, 60, and 70 °C, α-HBB is

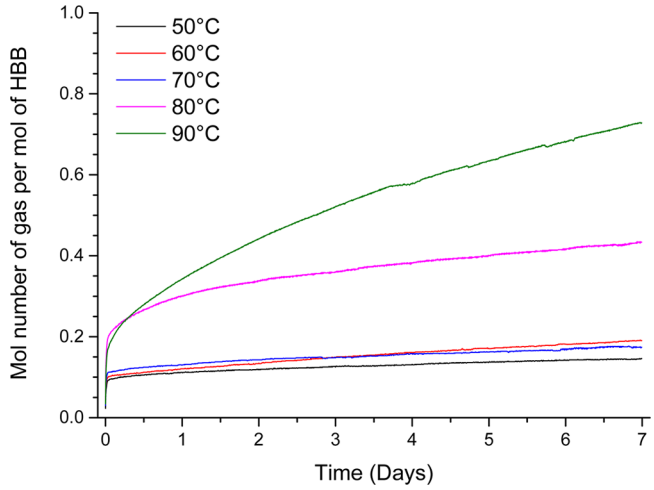

Figure 8. Thermolysis of α-HBB under isothermal conditions (50, 60, 70, 80, 90 °C): variation of the mole number of gas (H_2) per mole of α-HBB as a function of time (over 7 days).

rather stable, less than 0.2 mol of gas per mole of α-HBB being generated after 7 days. At 80 °C, 0.44 mol of gas evolved in our conditions. This is lower than the ca. 0.57 mol reported elsewhere at the same temperature but for a duration of only 12 h.[12] Reasons of such differences could be the sample purity and/or the experimental device; the difference of the crystal structure might be another reason. Anyway, our sample α-HBB is more stable. At 90 °C, our sample liberated 0.73 mol of gas per mole of α-HBB. Li et al. performed isothermal dehydrogenation measurements at higher temperatures, i.e., 80, 120, 135, and 150 °C.[12] They found 1.9, 2.8, 8.4, and 11 wt % H_2 released after 12 h, respectively. It is worth mentioning that these temperatures are lower than 160 °C, the temperature over which explosive decomposition was reported elsewhere[3] and herein. The data in Figure 8 were then exploited to

DOI: 10.1021/acs.inorgchem.5b00569
Inorg. Chem. 2015, 54, 4574−4583

determine the apparent activation energy of the decomposition of α-HBB (Figure S21, Supporting Information). The data from the curves obtained at 50 and 60 °C were not exploited because of the relative stability of the compound at these temperatures. The determination was performed with the data obtained at 70, 80, and 90 °C. An apparent activation energy of 112 ± 10 kJ mol^{-1} was found, and it is quite consistent with the energies mentioned in the previous paragraph, especially with the value reported by Sun et al. (106.4 kJ mol^{-1}).[11]

Solubility and Stability in Solution. The solubility in anhydrous tetrahydrofuran, which is the solvent used for the synthesis, was first determined to be 194.3 g L^{-1} or 3.254 mol L^{-1}. Hence, the volume of THF used for the synthesis (150 mL) is high enough to have a concentration below the solubility limit of HBB.

Like the counterparts ammonia borane and hydrazine borane,[19] the dehydrogenation of HBB could be envisaged by solvolysis (i.e., hydrolysis, methanolysis, and/or ethanolysis). Accordingly, we determined the solubility of HBB in protic solvents, water, methanol, and ethanol. We found 60.9 (1.020 mol L^{-1}), 94.1 (1.576 mol L^{-1}), and 91.5 g L^{-1} (1.532 mol L^{-1}), respectively. A solvolysis experiment (without catalyst) was then performed with each of these protic solvents. Typically, 50 mg of HBB was solved in 5 mL of solvent, and the hydrogen evolution was followed by using our solvolysis bench described elsewhere.[20] At 25 °C, less than 3, 3, and 2 mL of H_2 was generated over a period of 2 h.

The stability of HBB in protic solvents was also followed by solution-state $^{11}B\{^1H\}$ NMR for a storage period of 3 weeks, the samples being stored under inert atmosphere (in the glovebox). The spectra recorded after 3 weeks are shown in Figure 9. The quartets centered at −19.7, −18.2, and −18 ppm

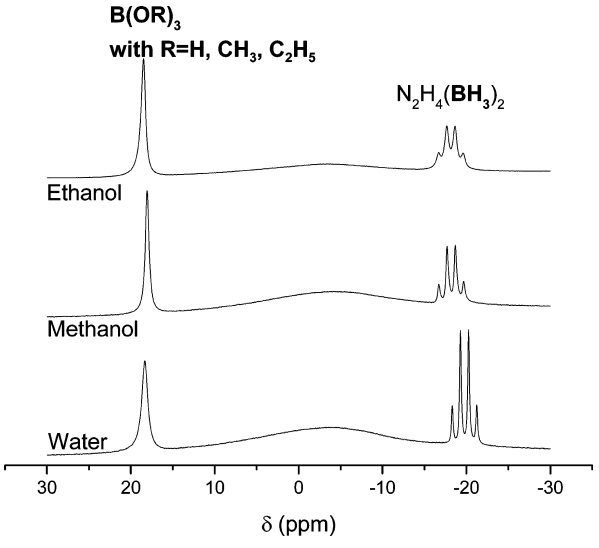

Figure 9. Solution-state ^{11}B NMR spectra of α-HBB solved in water, methanol, and ethanol after 3 weeks of storage under inert conditions.

for water, methanol, and ethanol as solvent, respectively, are ascribed to the BH_3 moiety of HBB. The singlets centered at 15.4, 18, and 18.6 ppm are attributed to B−O bond-containing products like $B(OH)_3$, $B(OCH_3)_3$, and $B(OC_2H_5)_3$.[21] These are evidence of the occurrence of the spontaneous solvolysis of HBB.

Discussion on Prospects for Chemical Hydrogen Storage. There is clearly a contradiction about the suitability of HBB for solid-state hydrogen storage implying dehydrogenation by thermolysis. After the first synthesis in 1967, violent explosion risk for rapid heating much beyond 100 °C was reported.[9] Forty years later, such a risk was confirmed while precision about the temperature was given (>160 °C).[3] The present work is a further confirmation. It also gives precisions about the conditions of explosion. With our lab-prepared HBB and in our experimental conditions, HBB exploded violently when heated at 10 °C min^{-1} and when the temperature reached 165 °C. Yet, such a risk was not reported in two recent studies while heating rates of 10 and 15 °C min^{-1} were applied.[11,12] At present, it is difficult to explain such an experimental contradiction. This may be rationalized by the sample purity and/or the experimental devices, but there is no sign to support these hypotheses.

After the first synthesis in 1967, the shock sensitivity of HBB was also reported.[9] A recent study confirmed this while stating that HBB "explodes even under mild ball-milling conditions".[17] In our laboratory, HBB was never ball milled in the pristine state. With the objective to prepare alkali (Li and Na) hydrazinidobisboranes, we ball milled HBB and LiH or NaH in various conditions, the most severe being 2 h of milling at 450 rpm for 2 min alternated with 5 min breaks. The synthesis of such derivatives failed systematically, with either no reactivity in soft/mild conditions or decomposition of HBB in severe conditions. No explosion occurred. Note that Fu et al. reported the successful synthesis of lithium hydrazinidobisborane $LiNH(BH_3)NH_2BH_3$ via the reaction between HBB and *n*-butyllithium in ether solution.[17]

Therefore, neat HBB would not be a suitable candidate for solid-state hydrogen storage. However, an alternative would be the elaboration of an alkali derivative,[17] since according to Fu et al.'s report there is no risk with $LiNH(BH_3)NH_2BH_3$, which besides shows better dehydrogenation properties. For this reason, HBB should not be discarded from the field. The situation is in fact similar to that of hydrazine borane and derivatives.[4,5]

Like the counterparts ammonia borane and hydrazine borane, HBB could be envisaged for dehydrogenation in solvolytic conditions, i.e., at temperatures between 20 and 50 °C. One argument in favor of that is related to the hydrogen content of HBB, which is higher than that of hydrazine borane. However, like for hydrazine borane, the attractiveness of HBB in this field will be strongly related to the ability to dehydrogenate the N_2H_4 moiety, since solvolysis of the BH_3 groups should be quite facile. The key material will then be the catalyst, for which activity toward the N_2H_4 moiety and selectivity for the release of 2 H_2 and 1 N_2 (instead of 4/3 NH_3 and 1/3 N_2) will be expected. We can reasonably think that the nickel-based catalyst already investigated for hydrazine borane could be equally effective.[20]

The stability of HBB in water, methanol, and ethanol is nevertheless not satisfactory. Like for sodium borohydride,[22] stabilization by hydroxide ions could be envisaged. Then the suitability of HBB in comparison to HB but also to ammonia borane and sodium borohydride could be more relevantly discussed.

■ CONCLUSION

Pure hydrazine bisborane was synthesized and completely characterized so that a complete data sheet gathering information on molecular and crystallographic structures, textural property and density, thermogravimetric and calori-

DOI: 10.1021/acs.inorgchem.5b00569
Inorg. Chem. 2015, 54, 4574−4583

metric behaviors, nature of the gas evolving under heating, solubility in protic solvents like water and methanol, and stability in solid and solution state. The analyses of the collected data helped in shedding light on the potential of hydrazine bisborane for chemical hydrogen storage. On one hand, pristine hydrazine bisborane is not suitable for solid-state chemical hydrogen storage because there is a risk of explosion in thermolysis conditions, especially at >150 °C and with a 10 °C min^{-1} heat ramp. However, the synthesis of alkali derivatives could be an alternative to the use of pristine hydrazine bisborane, and for this reason hydrazine bisborane is still a potential material in the field. On the other hand, aqueous hydrazine bisborane could be used for liquid-state chemical hydrogen storage, provided the molecule can be totally dehydrogenated in the presence of an active and selective metal-based catalyst. Alternatively, hydrazine bisborane could be used in the solid state and water provided in stoichiometric amounts. In fact, in hydrolytic conditions, hydrazine bisborane is richer in hydrogen than predecessors like sodium borohydride, ammonia borane, and hydrazine borane. In summary, hydrazine bisborane is another candidate for chemical hydrogen storage.

EXPERIMENTAL SECTION

HBB was prepared by using a slightly modified version of the protocol first described by Gunderloy.[9] Modifications were done by adapting the improvements we reported for the synthesis of hydrazine borane.[4] Typically, in an argon-filled glovebox (MBraun M200B, H_2O < 0.1 ppm, O_2 < 0.1 ppm), hydrazine sulfate ($[N_2H_5]^+[SO_4H]^-$, Sigma-Aldrich) and sodium borohydride ($NaBH_4$, Acros Organics) were separately and finely ground in agate mortars. This operation makes the reaction more efficient and the yield higher to some extent. The reactants (3.93 and 2.28 g, respectively) were transferred in a 250 mL three-necked round-bottom flask. The flask was put in the argon-vacuum line and in an oil bath set at 40 °C to avoid temperature variations during the reaction. Then 150 mL of anhydrous tetrahydrofuran (Sigma-Aldrich) was added with an argon-conditioned syringe two times (100 and 50 mL). The addition was performed under vigorous stirring. The reaction, with hydrogen evolution, started immediately. The outlet of the flask was connected to a bubble counter filled with paraffin oil via a water cooler and a flask used as a trap for the paraffin oil. The mixture was kept under stirring for 42−90 h at 40 °C, but higher yields were obtained for 90 h. The slurry was then filtrated. It is preferable not to wash the byproducts not to degrade the purity of HBB. Tetrahydrofuran was then removed (4 h for a solution kept at 25 °C), and the filtrate was dried under dynamic vacuum and room conditions for 24 h (with shorter times some tetrahydrofuran remain). In our optimized conditions, HBB was obtained with a yield of 87%. The sample was stored in the argon-filled glovebox and handled there. Its purity (>97%) was verified by ^1H (probe head dual $^1H/^{13}C$, 300.13 MHz, CD_3CN, 30 °C) and ^{11}B (probe head BBO10, 96.29 MHz, D_2O, 30 °C) solution-state nuclear magnetic resonance (NMR) on a Bruker AVANCE-300.

HBB is a finely divided white powder. Its specific surface area was determined by N_2 adsorption/desorption (Micromeritics, ASAP-2020). The sample degassing was performed in room conditions in order to avoid any unwanted decomposition at higher temperatures. Its density was measured by helium pycnometer (Micromeritics, Accupyc 1330), also to compare to the value obtained from the crystallographic cell data. The analysis was performed twice, with two different samples (<1 g). The datum for the first one was repeated 7 times while that of the second one 6 times. An error of 4 g cm^{-3} was calculated from the 13 data. Note that HBB shows electrostatic behavior, which makes its handling and transfer into vials sometimes difficult.

The molecular structure of HBB was analyzed by solution-state (cf. above) and solid-state ^{11}B MAS NMR (Varian VNMR400, ^1H 400 MHz, ^{11}B 128.37 MHz, −10 °C, 18500 rpm) and Fourier transform infrared spectroscopy (IR, Nicolet 710, 128 scans). Raman measurements were carried out at 25 °C using a confocal microspectrometer (Labram HR, Jobin-Yvon) and a sealed tube. The sample volume was illuminated using a diode laser beam (659.55 nm) focused by an objective (*50LF, N.A=0.5, Olympus). The scattered light was collected using the same objective and dispersed with a 1 cm^{-1} spectral resolution using a grating of 1800 lines mm^{-1}. The axial resolution of the confocal height was around 12 μm in our optical configuration. The Raman signal was detected with a CCD (charge-coupled device) system.

Powder X-ray diffraction was carried out on Swiss Norvegian Beamlines at the European Synchrotron Radiation Facility (ESRF, Grenoble, France). The diffraction patterns were collected using a monochromatic beam with a wavelength of 0.70814 Å and PILATUS 2 M detector. The sample−detector distance (343.71 mm) and parameters of the detector were calibrated using NIST standard LaB6. Two-dimensional diffraction images were integrated using Fit2D software.[23] A fine powder of HBB was loaded into a glass capillary of 0.5 mm diameter into a glovebox and then sealed. The capillaries were cooled from room temperature to −193 °C and then heated at 30 °C/h up to −23 °C, while synchrotron powder-diffraction data were collected in situ. The temperature was controlled with an Oxford Cryostream 700+. During each collection time (120 s per image), the capillary was rotated by 60° in the same angular interval. The powder patterns were indexed using DICVOL06,[24] and the structures were fully determined using FoX and the Jana2006 software package.[25]

The behavior of HBB under heating was analyzed by thermogravimetric analysis (TGA) with TGA Q500 (TA Instruments). The following conditions were applied: sample mass of ca. 3 mg, aluminum crucible of 40 mL with a pinhole, routine heating rate of 5 °C min^{-1}, temperature range of 40−400 °C, and atmosphere of N_2 (60 mL min^{-1}). Slower (1 and 3 °C min^{-1}) and faster (10 °C min^{-1}) heating rates were also envisaged. Another TGA apparatus (Rigaku TG8120), to which was coupled a mass spectrometer (MS; M-QA200TS), was employed to perform gas analysis. HBB was also analyzed by differential scanning calorimetry (DSC; TA Instruments, 2920 MDSC) in experimental conditions that were identical to those used for the TGA measurements. Note that unlike ammonia borane and hydrazine borane, no swelling, due to melting and subsequent gas evolution, was observed. This is consistent with Gunderloy's observation (i.e., no melting up to 100 °C).[9] The decomposition of HBB under isothermal conditions was investigated at four temperatures: 50, 60, 70, 80, and 90 °C. Typically, ca. 100 mg of material was introduced into a stainless steel reactor (50 mL) in the argon-filled glovebox. The reactor was then immersed in an oil bath kept at the desired temperature. The variation of pressure in the reactor was then followed with time and simultaneously recorded on an MS Excel file. The pressure variation was subsequently transformed into a mole number and plotted as a function of time.

The stability of HBB in anhydrous tetrahydrofuran (Sigma-Aldrich), deionized water (Millipore milli-q water, with a resistivity >18 MΩ cm), methanol (Sigma-Aldrich), and ethanol (Sigma-Aldrich), under an argon atmosphere, was studied by solution-state ^{11}B NMR over 3 weeks. The solutions were prepared in NMR tubes in the glovebox, and a coaxial tube containing deuterated water D_2O was inserted in the tubes, which were then hermetically sealed.

COMPUTATIONAL METHODS

Computational methods were used to probe the structural properties of HBB. A first strategy was to consider molecular calculations. Indeed, the molecular structure of the borane was determined from an energy minimization by means of density functional theory (DFT) simulations implemented in DMol^3.[26] These calculations were performed considering the PW91 GGA density functional,[27] the double numerical basis set containing polarization functions on hydrogen atoms (DNP), and all electrons for the core treatment. The criteria leading to the convergence of the calculations were fixed at the fine level (10^{-5} Ha for energy, 0.002 Ha/Å for maximal force, 0.005 Å

DOI: 10.1021/acs.inorgchem.5b00569
Inorg. Chem. 2015, 54, 4574−4583

for maximal displacement). The partial charges for the molecule were calculated by the ESP charge partitioning method.[28] From this molecular structure, the NMR, Raman, and FTIR spectra were calculated using CASTEP,[29] a DFT-based code using the projector-augmented waves (PAW) and gauge-included projector-augmented waves (GIPAW) algorithms for the EFGs and NMR chemical shifts, respectively. Here, the PBE functional was used in the generalized gradient approximation (GGA) for the exchange correlation energy.[30] The core−valence interactions were described by ultrasoft pseudopotentials.[31] The pseudopotentials generated "on the fly" within the NMR CASTEP package were used, without implemention of any additional corrections. In contrast, the "Norm conserving" pseudopotentials were used as imposed in CASTEP for the calculations of Raman spectra. The wave functions were expanded on a plane wave basis set with a kinetic energy cutoff of 440 eV. The computations were performed on the optimized molecular structure. Such approach was been used in analogous solids.[32] Similar calculations with Gaussian09 were performed to compare both NMR shielding and Raman/FTIR spectra. In this case, the 6-311G++ basis set with (2d, 3p) polarization functions and B3LYP exchange-correlation function were chosen. The comparison of the structures obtained with the different codes leads to very similar structures. A second strategy, i.e., periodic calculations, was used to probe the structural/periodic and molecular properties of HBB. Periodic structures were built using the experimental unit cell parameters extracted from the XRD measurements at different temperatures (low and room temperatures). The effect of the temperature was thus taken into account through these unit cell parameters kept as fixed during DFT calculations. The HBB molecules already optimized were placed in the network and geometry optimized again with CASTEP code, allowing us to compare both periodic and molecular structures. In the latter case, the effect of neighbors could be investigated in contrast with molecular structure in which only one HBB molecule was considered. Molecule geometry, NMR shielding, and Raman spectra were extracted from similar calculations described in the molecular calculations part.

■ ASSOCIATED CONTENT

Supporting Information

Figures, tables, and details about the results of the computational calculations. This material is available free of charge via the Internet at http://pubs.acs.org.

■ AUTHOR INFORMATION

Corresponding Author

*Phone: +33 4 67 14 91 60. Fax: +33 4 67 14 91 19. E-mail: umit.demirci@um2.fr.

Author Contributions

The manuscript was written through contributions of all authors. All authors have given approval to the final version of the manuscript.

Notes

The authors declare no competing financial interest.

■ ACKNOWLEDGMENTS

We thank the European Synchrotron Radiation Facility and the Swiss Norvegian Beamline (BM01A) for the beam time allocation. We also thank MSc. A. Ballestero (Univ. Montpellier) for the density determination by pycnometry and Prof. T. Ichikawa (Hiroshima Univ.) for access to TGA-MS. P.G.Y. thanks Prof. J. C. Tedenac and Dr. J. Haines (ICGM) for fruitful discussions on crystal structure determination.

■ DEDICATION

This article is dedicated to Jean-Pierre RAVIER (IEM), wishing him a happy retirement.

■ REFERENCES

(1) Li, C.; Peng, P.; Zhou, D. W.; Wan, L. *Int. J. Hydrogen Energy* **2011**, *36*, 14512−14526.

(2) (a) Dietrich, B. L.; Goldberg, K. I.; Heinekey, D. M.; Autrey, T.; Linehan, J. C. *Inorg. Chem.* **2008**, *47*, 8583−8585. (b) Sloan, M. E.; Clark, T. J.; Manners, I. *Inorg. Chem.* **2009**, *48*, 2429−2435. (c) Staubitz, A.; Robertson, A. P. M.; Manners, I. *Chem. Rev.* **2010**, *110*, 4079−4124. (d) Hügle, T.; Hartl, M.; Lentz, D. *Chem.—Eur. J.* **2011**, *17*, 10184−10207. (e) Wang, P. *Dalton Trans.* **2012**, *41*, 4296−4302.

(3) Hügle, T.; Kühnel, M. F.; Lentz, D. *J. Am. Chem. Soc.* **2009**, *131*, 7444−7446.

(4) Moury, R.; Moussa, G.; Demirci, U. B.; Hannauer, J.; Bernard, S.; Petit, E.; van der Lee, A.; Miele, P. *Phys. Chem. Chem. Phys.* **2012**, *14*, 1768−1777.

(5) (a) Wu, H.; Zhou, W.; Pinkerton, F. E.; Udovic, T. J.; Yildirim, T.; Rush, J. J. *Energy Environ. Sci.* **2012**, *5*, 7531−7535. (b) Moury, R.; Demirci, U. B.; Ichikawa, T.; Filinchuk, Y.; Chiriac, R.; van der Lee, A.; Miele, P. *Chem. Sus. Chem.* **2013**, *6*, 667−673. (c) Chua, Y. S.; Pei, Q.; Ju, X.; Zhou, W.; Udovic, T. J.; Wu, G.; Xiong, Z.; Chen, P.; Wu, H. *J. Phys. Chem. C* **2014**, *118*, 11244−11251. (d) Moury, R.; Demirci, U. B.; Ban, V.; Filinchuk, Y.; Ichikawa, T.; Zeng, L.; Goshome, K.; Miele, P. *Chem. Mater.* **2014**, *26*, 3249−3255. (e) Moury, R.; Petit, J. F.; Demirci, U. B.; Ichikawa, T.; Miele, P. *Int. J. Hydrogen Energy* **2015**, DOI: 10.1016/j.ijhydene.2015.01.053.

(6) Kipichev, E. B.; Rubisov, Yu. I.; Marelis, G. B. *Russ. J. Inorg. Chem.* **1971**, *16*, 1102−1103.

(7) Emeléus, H. J.; Stone, F. G. A. *J. Chem. Soc.* **1951**, 840−841.

(8) Steindler, M. J.; Schlesinger, H. I. *J. Am. Chem. Soc.* **1953**, *75*, 756−756.

(9) Gunderloy, F. C., Jr. *Inorg. Synth.* **1967**, *9*, 13−16.

(10) (a) Sayles, D. C. Compacted hydrazine bisborane fuel and method of operating gas generators. U.S. Patent 3170283, 1965. (b) Bratton, F. H.; Reynolds, H. I. Hydrogen generating system. U.S. Patent 3419361, 1968;. (c) Coleman, J. E. Stabilized hydrazine bisborane. U.S. Patent 3382050, 1968. (d) Longwell, J. P. Rocket nozzle cooling. U.S. Patent 3521452, 1970;. (e) Olsen, R. N. Monopropellant in binder matrix. U.S. Patent 3499289, 1970. (f) Grant, L. R.; Flanagan, J. E. Advanced solid reactant for H_2/D_2 generation. U.S. Patent 4381206, 1983.

(11) Sun, W.; Gu, Q.; Guo, Y.; Guo, Z.; Liu, H.; Yu, X. *Int. J. Hydrogen Energy* **2011**, *6*, 13640−13644.

(12) Li, L.; Tan, Y. Z.; Tang, Z.; Xia, G.; Yuan, F.; Li, Q.; Yu, X. *Mater. Chem. Phys.* **2014**, *143*, 1055−1060.

(13) (a) Shore, S. G.; Chen, X. Methods for synthesizing ammonia borane. U.S. Patent 2009/0104102, 2009. (b) Heldebrant, D. J.; Karkamkar, A.; Linehan, J. C.; Autrey, T. *Energy Environ. Sci.* **2008**, *1*, 156−160. (c) Basu, S.; Zheng, Y.; Gore, J. P. *J. Power Sources* **2010**, *196*, 734−740.

(14) (a) Berl, W. G.; Wilson, W. R. *Nature* **1961**, *191*, 380−380. (b) Smith, J.; Seshardri, K. S.; White, D. *J. Mol. Spectrosc.* **1973**, *45*, 327−337. (c) Nguyen, V. S.; Swinnen, S.; Leszczynski, J.; Nguyen, M. T. *Phys. Chem. Chem. Phys.* **2011**, *13*, 6649−6656. (d) Thomas, J.; Klahn, M.; Spannenberg, A.; Beweries, T. *Dalton Trans.* **2013**, *42*, 14668−14672.

(15) (a) Trudel, S.; Gilson, D. F. R. *Inorg. Chem.* **2003**, *42*, 2814−2816. (b) Heldebrant, D. J.; Karkamkar, A.; Hess, N. J.; Bowden, M.; Rassat, S.; Zeng, F.; Rappe, K.; Autrey, T. *Chem. Mater.* **2008**, *20*, 5332−5336. (c) Liu, A.; Song, Y. *J. Phys. Chem. C* **2012**, *116*, 2123−2131. (d) He, T.; Wu, H.; Chen, J.; Wu, G.; Xiong, Z.; Zhang, T.; Chen, P. *Phys. Chem. Chem. Phys.* **2013**, *15*, 10487−10493.

(16) Mebs, S.; Grabowsky, S.; Förster, D.; Kickbusch, R.; Hartl, M.; Daemen, L. L.; Morgenroth, W.; Luger, P.; Paulus, B.; Lentz, D. *J. Phys. Chem. A* **2010**, *114*, 10185−10196.

DOI: 10.1021/acs.inorgchem.5b00569
Inorg. Chem. 2015, 54, 4574−4583

(17) Fu, H.; Yang, J.; Wang, X.; Xin, G.; Zheng, J.; Li, X. *Inorg. Chem.* **2014**, *53*, 7334−7339.
(18) Kissinger, H. E. *Anal. Chem.* **1957**, *29*, 1702−1706.
(19) Yadav, M.; Xu, Q. *Energy Environ. Sci.* **2012**, *5*, 9698−9725.
(20) (a) Clémençon, D.; Petit, J. F.; Demirci, U. B.; Xu, Q.; Miele, P. *J. Power Sources* **2014**, *260*, 77−81. (b) Ben Aziza, W.; Petit, J. F.; Demirci, U. B.; Xu, Q.; Miele, P. *Int. J. Hydrogen Energy* **2014**, *39*, 16919−16926.
(21) Hannauer, J.; Demirci, U. B.; Pastor, G.; Geantet, C.; Herrman, J. M.; Miele, P. *Energy Environ. Sci.* **2010**, *3*, 1796−1803.
(22) (a) Demirci, U. B.; Akdim, O.; Andrieux, J.; Hannauer, J.; Chamoun, R.; Miele, P. *Fuel Cells* **2010**, *10*, 335−350. (b) Muir, S. S.; Yao, X. *Int. J. Hydrogen Energy* **2011**, *36*, 5983−5997. (c) Santos, D. M. F.; Sequeira, C. A. C. *Renew. Sust. Energy Rev.* **2011**, *15*, 3980−4001.
(23) Hammersley, A. P.; Svensson, S. O.; Hanfland, M.; Fitch, A. N.; Häusermann, D. *High Press. Res.* **1996**, *14*, 235−248.
(24) Boultif, A.; Louer, D. *J. Appl. Crystallogr.* **1991**, *24*, 987.
(25) (a) Favre-Nicolin, V.; Černý, R. *J. Appl. Crystallogr.* **2002**, *35*, 734. (b) Petricek, V.; Dusek, M.; Palatinus, L. *Jana2006*; Institute of Physics: Praha, Czech Republic, 2006.
(26) *DMol3*; Accelrys Inc.: San Diego CA, 2008.
(27) Perdew, J. P.; Wang, Y. *Phys. Rev. B* **1992**, *45*, 13244−13249.
(28) Singh, C. U.; Kollman, P. A. *J. Comput. Chem.* **1984**, *5*, 129−145.
(29) Segall, M. D.; Lindan, P. L. D.; Probert, M. J.; Pickard, C. J.; Hasnip, P. J.; Clark, S. J.; Payne, M. C. *J. Phys.: Condens. Matter* **2002**, *14*, 2717−2744.
(30) Perdew, J. P.; Burke, K.; Ernzerhof, M. *Phys. Rev. Lett.* **1996**, *77*, 3865−3868.
(31) Yates, J. R.; Pickard, C. J.; Mauri, F. *Phys. Rev. B* **2007**, *76* (024401), 1−11.
(32) Lingam, C. B.; Babu, K. R.; Tewari, S. P.; Vaitheeswaran, G. *J. Comput. Chem.* **2011**, *32*, 1734−1742.

DOI: 10.1021/acs.inorgchem.5b00569
Inorg. Chem. 2015, 54, 4574−4583